Published in final edited form as:
NMR Biomed. 2012 April ; 25(4): . doi:10.1002/nbm.1767.

T_2 measurement of J-coupled metabolites in the human brain at 3T

Sandeep K. Ganji[a], **Abhishek Banerjee**[a], **Aditya M. Patel**[a], **Yan D. Zhao**[b,c], **Ivan E. Dimitrov**[a,d], **Jeffrey D. Browning**[e], **E. Sherwood Brown**[f], **Elizabeth A. Maher**[g], and **Changho Choi**[a,h,*]

[a]Advanced Imaging Research Center, University of Texas Southwestern Medical Center, Dallas, Texas, USA

[b]Department of Clinical Sciences, University of Texas Southwestern Medical Center, Dallas, Texas, USA

[c]Harold C. Simmons Cancer Center, University of Texas Southwestern Medical Center, Dallas, Texas, USA

[d]Philips Medical Systems, Cleveland, Ohio, USA

[e]Department of Internal Medicine, University of Texas Southwestern Medical Center, Dallas, Texas, USA

[f]Department of Psychiatry, University of Texas Southwestern Medical Center, Dallas, Texas, USA

[g]Departments of Internal Medicine and Neurology, University of Texas Southwestern Medical Center, Dallas, Texas, USA

[h]Department of Radiology, University of Texas Southwestern Medical Center, Dallas, Texas, USA

Abstract

The proton T_2 relaxation times of metabolites in the human brain were measured using point-resolved spectroscopy at 3T *in vivo*. Four echo times (54, 112, 246 and 374 ms) were selected from numerical and phantom analyses for effective detection of the glutamate multiplet at ~2.35 ppm. *In vivo* data were obtained from medial occipital and left occipital cortices of five healthy volunteers, which contained predominantly gray and white matter, respectively. Spectra were analyzed with LCModel software using volume-localized calculated spectra of brain metabolites. The estimate of the signal strength *vs.* TE was fitted to a monoexponential function for estimation of apparent T_2 ($T_2^{\dagger}$). The $T_2^{\dagger}$ was estimated to be similar between the brain regions for creatine, choline, glutamate and myo-inositol, but significantly different for the N-acetylaspartate singlet and multiplet. The $T_2^{\dagger}$s of glutamate and myo-inositol were measured as 181±16 and 197±14 ms (mean±SD, N = 5) for medial occipital, and 180±12 and 196±17 ms for left occipital, respectively.

Keywords

^{1}H-MRS; Relaxation time (T_2); J-coupled metabolites; 3T; Human brain; Gray matter; White matter

[*]**Correspondence to:** Changho Choi, Ph.D, Phone: 214-645-2805, FAX: 214-645-2885, changho.choi@utsouthwestern.edu.

INTRODUCTION

Proton MRS offers a noninvasive tool for measuring metabolites in the human brain *in vivo*. While measurement with short TE benefits from minimum T_2 signal loss, long-TE approaches are often employed as an alternative (1–3), with advantages that TE optimization can improve the spectral resolution and the uncertainties of metabolite measures due to broad baseline signals from macromolecules are reduced. The detected signals are, however, T_2 weighted and thus may not reflect the metabolite concentrations directly. T_2 relaxation may reflect the cellular and molecular environments of metabolites in the brain; *e.g.*, viscosity of the cellular fluids and microscopic susceptibility distribution within cells (4,5). Increased T_2 relaxation could occur due to reduced cell volumes and altered micromolecule structures in bipolar disorder and schizophrenia (6). A reasonable estimate of metabolite T_2 may therefore be valuable not only for quantification of the metabolite levels but also for understanding the physiological and pathological changes in disease conditions.

Most of prior studies of T_2 measurements for metabolites in the human brain focused on prominent singlet signals, such as N-acetylaspartate (NAA), total creatine (tCr), and total choline (7–15). While the TE dependence of a singlet is described by T_2 relaxation only, the time evolution of scalar coupled metabolite signals is affected by the effects of the J evolution as well as T_2 relaxation. Measurements of relaxation times of coupled resonances therefore require proper evaluation of the J evolution on the signals (16,17). The primary excitatory neurotransmitter glutamate (Glu) and the glial marker myo-inositol (mIns) are measured in many clinical studies (18). The complex behavior of the multiplets with changing TE, which occurs due to strong coupling effects, makes it difficult to measure the T_2 relaxation times *in vivo*. Moreover, when the bandwidth of the spatially localizing RF pulses are not much greater than the spectral distance between coupled resonances, non-uniform coherence distribution within the localized volume arises from chemical shift localization errors (19), resulting in complicated behavior of the multiplets with changing TE. Due to these spectral complexities, there is paucity in reports of T_2 relaxation times of coupled-spin metabolites.

Due to its single-shot volume-localization full-refocusing capability, point-resolved spectroscopy (PRESS) is widely used in clinical studies. The *in vivo* evaluation of brain metabolite T_2 may depends on MRS sequence. As shown by Michaeli *et al*. (11), signal reduction due to the molecular diffusion effects may result in reduced T_2 estimates ($T_2^{\dagger}$) when measured with PRESS, compared to Carr Purcell-type sequences. Thus, signal reduction with increasing TE may be greater in PRESS than in sequences with increased number of 180° RF pulses. Thus, the Glu T_2 values obtained using a triple-refocusing method (16) may not be directly applicable to PRESS measures of Glu at intermediate or long TEs. Given the field dependence of metabolite T_2 measures (11) and the utility of long-TE approaches for measurements of J-coupled metabolites at 3T, a field strength increasingly available for *in vivo* spectroscopy, measurement of $T_2^{\dagger}$ of coupled metabolites by PRESS at 3T is of high significance.

Here, we report measurements of apparent proton T_2 relaxation times ($T_2^{\dagger}$) of metabolites in the human brain at 3T, using a PRESS sequence. The metabolites include Glu, mIns, NAA aspartate (Asp) moiety, and N-acetylaspartylglutamate (NAAG), in addition to tCr, NAA and choline singlets. Four echo times in the range 50–400 ms were selected from computer simulations that incorporated the shaped RF and gradient pulses, and validated in phantoms. *In vivo* results from the gray- and white-matter dominant occipital regions in five healthy volunteers are presented.

MATERIALS AND METHODS

Experiments were carried out on a 3.0 T whole-body Philips scanner with actively shielded gradient coils (maximum gradient strength 80 mT/m; slew rate 200 mT/m/ms) (Philips Medical Systems, Best, The Netherlands). An integrated body coil was used for RF transmission and an eight-channel phased-array head coil for signal reception. A PRESS sequence was used for measurement of apparent T_2 ($T_2^\dagger$) of brain metabolites; 90 – $TE_1/2$ – 180 – $TE_1/2$ – $TE_2/2$ – 180 – $TE_2/2$ – Acquisition. Single-voxel localization was obtained with a 9.8-ms amplitude/frequency-modulated 90° RF pulse (bandwidth = 4.25 kHz) and 13.2-ms amplitude-modulated 180° RF pulses (bandwidth = 1.27 kHz), the same RF envelopes used as in a prior study (20). A vendor-set maximum allowed RF field intensity (B_1 = 13.5 μT) was used for the RF pulses. The slice selection was obtained along the anterior-posterior, left-right, and foot-head directions using the 90° and the first and second 180° RF pulses, respectively, for which the gradient strength was 4.0 and 1.0 mT/m for slice thickness of 25 and 30 mm, respectively. A pair of spoiling gradients (3.5 ms long; 20 mT/m) was applied in the same direction as that of the slice selective gradient for each 180° pulse.

Four pairs of PRESS subecho times were used for $T_2^\dagger$ measurement; (TE_1, TE_2) = (32, 22), (32, 80), (32, 214), and (36, 338) ms. Here, the echo time pair (32, 22) ms was the shortest possible for the chosen RF and gradient pulses. The other three TE_1-TE_2 pairs were obtained from density-matrix simulations, largely focusing on Glu. The C4-proton multiplet of glutamate was varied with changing TE due to the J coupling effects, giving relatively large and positive signals at TE = ~110, ~250, and ~370 ms, for which the subecho times were asymmetric ($TE_1 \neq TE_2$). We chose subecho time pairs with $TE_1 < TE_2$ because residual eddy current artifacts may be less in these pairs than in $TE_1 > TE_2$. The simulations were performed including the effects of the shaped RF and gradient pulses as well as the Zeeman, chemical shift and J coupling effects, thus the effects of the finite bandwidth of volume selective RF pulses are accounted for precisely. Published chemical shift and coupling constants were used in the simulation (18). The simulations were programmed with Matlab (The MathWorks Inc., Natick, MA, USA).

The optimized PRESS echo times were tested in an aqueous solution (pH = 7.2) with Cr (8 mM), Glu (20 mM), and Gln (20 mM). Phantom spectra were obtained from a 25×25×25 mm^3 voxel, using a TR of 10 s (> $5T_1$), and compared with numerically-calculated spectra.

In vivo measurement of brain metabolite $T_2^\dagger$ was conducted in five healthy volunteers (2 female and 3 male; age 27±7 years). The protocol was approved by the Institutional Review Board of the University of Texas Southwestern Medical Center. Written informed consent was obtained prior to the scans. Following survey scans, T_1-weighted images (MP-RAGE) were acquired (TR/TE/TI = 2500/3.7/1300 ms; flip angle = 8°; field of view = 240×240×150 mm; 150 slices; resolution = 1×1×1 mm^3). Spectroscopic data were obtained from the medial occipital and left occipital regions (voxel size 25×30×30 mm^3), which are predominantly gray- and white-matter, respectively. The number of averages was 16, 32, 64, and 128 for the four TEs, respectively, to compensate for the SNR loss at longer TEs, similarly to the prior study (12). First- and second-order shimming for the selected volume was carried out using the fast automatic shimming technique by mapping along projections (FASTMAP) (21). The linewidth of the water signal was ~7 Hz at TE = 54 ms. Data acquisition parameters included; TR = 3 s, sweep width = 2.5 kHz, and sampling points = 2048. Following 6 dummy scans, signals were recorded in multiple blocks, each with 4 averages. A 64-step phase cycling scheme was used for the PRESS data acquisition. The carriers of slice-selective RF pulses were set at 3 ppm. A four-pulse variable-flip-angle scheme was used for water suppression. Unsuppressed brain water signals were acquired at

the four TEs with the same gradient schemes as those of water-suppressed acquisitions. The total MR scan time was ~1 hr including the shimming, power calibration, and water imaging times.

The multi-block data were processed individually for correction of eddy current artifacts and frequency drifts using an in-house written MATLAB program. Residual eddy current effects were minimized using the unsuppressed brain water signal. The frequency drifts were corrected using the NAA singlet as a reference. Data were apodized with a 1-Hz exponential function for enhancing SNR and removing potential artifacts in the later part of FID. Spectral fitting was performed using the LCModel software (22). 3D volume localized model spectra of brain metabolites were numerically calculated and used as a basis function for the fitting. The basis function included 18 metabolites; tCr, NAA, Glu, mIns, GABA, NAAG, GPCPC (glycerophosphocholine + phosphocholine), Gln (glutamine), GSH (glutathione), glycine, taurine, scyllo-inositol, acetate, aspartate, phosphoethanolamine, ethanolamine, lactate, and threonine. Given the potential differences in relaxation times between resonances within a metabolite, model spectra were created individually for subgroups of the metabolite according to their coupling connections. These metabolites included tCr (methyl and methylene groups), NAA (acetyl and aspartate moieties), NAAG (acetyl, aspartyl, and glutamate moieties), and GSH (glycine, cysteine, and glutamate moieties). The spectral fitting range was set to 0.5 – 4.1 ppm. Cramér-Rao lower bounds (CRLB), which represent the lower bound of precision, were returned as a percentage standard deviation (%SD) with respect to the signal estimates. The LCModel estimates of signal strengths at the four echo times were fitted with a monoexponential function, $exp(-TE/T_2^{\dagger})$. The fitting was performed on LCModel estimates with CRLB less than 20% at all the four TEs. The T_1-weighted images were segmented, using Statistical Parametric Mapping software (SPM5), to obtain the fractions of gray matter (GM), white matter (WM), and cerebrospinal fluids (CSF) within the voxels.

RESULTS

Figure 1 presents comparison between numerically calculated (sum) and phantom spectra of Glu, Cr3 (Cr-CH_3) and Cr2 (Cr-CH_2) for the four pairs of PRESS subecho times, together with a calculated spectra of individual metabolites. The signal strength and spectral pattern of Glu and Gln varied with changing echo time due to the J evolution of the coupled resonances. The echo time dependence of the multiplets was in good agreement between calculation and experiment for both Glu and Gln. The Glu multiplet pattern was well preserved at the optimized echo times (except for (TE_1, TE_2) = (32, 22) ms). These simulation results were reproduced in phantom spectra, with phantom $T_2^{\dagger}$s of Glu, Gln, Cr-CH_3 and Cr-CH_2 at 720, 660, 1190 and 890 ms, respectively.

Figure 2 presents *in vivo* spectra from medial occipital and left occipital cortices of 5 subjects enrolled in the study, obtained at the four pairs of PRESS subecho times, together with voxel positioning (voxel size 25×30×30 mm^3). The spectra from the 5 subjects showed similar pattern for each voxel, indicating consistent voxel positioning between the subjects. The spectral patterns in the 2.2 – 2.5 ppm and 3.4 – 3.65 ppm regions, which were largely attributed to Glu and mIns, respectively, showed good agreement between the subjects. The GPCPC singlet intensity was quite different between the regions, likely due to differences in gray and white matter contents within the voxels. The GPCPC singlet at 3.2 ppm was about 50% the tCr-CH_3 singlet at TE = 54 ms. This signal ratio increased with TE and their signal strengths were similar at TE = 374 ms, indicating a long $T_2^{\dagger}$ of GPCPC compared to that of tCr. Segmentation of T_1-weighted images gave mean fractions of GM, WM and CSF as 60±3, 25±2 and 15±1% for medial occipital, and 16±2, 74±4 and 10±2% for left occipital, respectively. Figure 3 displays *in vivo* spectra at the four PRESS TEs from the medial and

left occipital cortices of a healthy subject (subject 1 in Fig. 2), together with LCModel fits and residuals. The spectra were all well reproduced by the fits, resulting in residuals without considerable dependence on chemical shift resonance. Due to the increased number of signal averages at the longer TEs (16, 32, 64 and 128 for TE = 54, 112, 246 and 374 ms, respectively), the residuals were progressively smaller with increasing TE.

Monoexponential fitting for metabolite $T_2^\dagger$ estimation was performed for LCModel estimates at the four TEs that had CRLBs less than 20%. The fitting included the multiplets of Glu, mIns, the NAA-Asp moiety, and the NAAG singlet, in addition to the three prominent signals, *i.e.*, the singlets of tCr (3.03 ppm), NAA (2.01 ppm) and GPCPC (3.2 ppm). The CRLB of Glu was 2 - 4% at TE = 54, 112 and 246 ms, and 4 – 5% at TE = 374 ms for both brain regions, as shown in Fig. 4a. The mIns CRLBs were somewhat larger, the mean values being 4, 4, 6 and 9% at TE = 54, 112, 246 and 374 ms, respectively (Fig. 4). The mean CRLBs of NAA-Asp were 3, 4, 4 and 5% at the four TEs, respectively. For the NAAG singlet, only the data from the left occipital region gave CRLBs less than 20% at the four TEs (*i.e.*, mean values were 6, 7, 7 and 8, respectively). Compared to left occipital, the data from medial occipital gave much greater CRLBs. The CRLBs were less than 20% only at TEs shorter than 374 ms, at which NAAG estimates were not reliable (CRLB > 50). The NAAG $T_2^\dagger$ fitting was therefore performed for left occipital only. The methyl group proton signals of tCr, NAA and GPCPC were all well defined, giving CRLBs less than 3% at all TEs. Figure 4b presents the correlation coefficients between the estimates of Glu and several metabolites having resonances adjacent to the Glu signals. While Glu and Gln showed more or less negative correlations at TE = 246 and 374 ms, the two short TEs gave positive correlations between the metabolites, implying that the Glu and Gln estimation could be influenced by other metabolites, which may include GABA, GSH and macromolecules. At TE = 54 ms, the macromolecule signals may not be attenuated completely, but since the Glu and Gln C4-proton multiplets were not extensively overlapped as indicated in Fig. 1, the covariance between Glu and Gln were similar at TE = 54 and 112 ms. The correlation coefficients of Glu with respect to other resonances were more or less within ±0.5 at the four TEs, indicating that the Glu signals were estimated without substantial uncertainties due to the neighboring interferences, which may provide Glu T_2 estimation with acceptable precision.

Figure 5 illustrates monoexponential fittings for several metabolite signals for the spectra from subject 1 shown in Fig. 2. The upper panel shows fits of major singlet signals (*i.e.*, tCr-CH_3tCr-CH_2NAA and GPCPC) and the lower panel shows Glu, mIns, NAA-Asp, and NAAG. The signal decay *vs*. TE was well represented by a monoexponential function, giving coefficients of determination (R^2) of monoexponential fitting close to unity. Table 1 shows mean $T_2^\dagger$ and R^2 of the metabolites and *p* values from paired t-tests (uncorrected and Bonferroni corrected) for the $T_2^\dagger$ values between the medial occipital and left occipital regions. The $T_2^\dagger$ of Glu was measured to be 181±16 and 180±12 ms (mean±SD, N = 5) for medial occipital and left occipital, respectively. The mIns $T_2^\dagger$ was estimated as 197±14 and 196±17 ms, respectively. For these coupled-spin metabolites, the $T_2^\dagger$ was measured to be very similar between the two regions ($p > 0.8$). The Glu and mIns data were well fitted with a monoexponential function for both regions, with $R^2 \approx 0.99$ and 0.97, respectively. The $T_2^\dagger$s of tCr-CH_3tCr-CH_2 and GPCPC were measured to be ~150, ~120 and ~230 ms for both regions, respectively. The $T_2^\dagger$ of the NAA singlet was observed to be ~260 and ~310 ms for medial occipital and left occipital, respectively. The difference was statistically significant ($p = 0.008$; paired t-test). The $T_2^\dagger$ of the NAA-Asp CH_2 resonances was also observed to be quite different between the regions (~220 and ~280 ms, respectively; $p = 0.009$). The reliability of the $T_2^\dagger$ fitting of this NAA multiplet was low, as indicated by large standard deviations and relatively small R^2 values. The *p*-values from Bonferroni correction for NAA and NAA-Asp were close to 0.05, indicating statistical evidence for the presence

of relaxation time differences between the two regions. The $T_2^\dagger$ of the NAAG singlet was measured as ~290 ms for the left occipital region, with mean R^2 of 0.934. In addition, the brain water $T_2^\dagger$ was estimated using the unsuppressed water signals acquired with PRESS. The water signals did not exhibit a monoexponential TE dependence consistently, primarily due to the long T_2 effects of the CSF water. Thus, the water signals at TE = 54, 112, and 246 ms only were used for $T_2^\dagger$ estimation, giving $T_2^\dagger$ of ~83 ms for both medial and left occipital, as shown in Table 1.

DISCUSSION

The present study reports apparent T_2 values of brain metabolites, including Glu, mIns, NAA-Asp, and NAAG, in addition to the major singlets. The signal intensity and spectral pattern of coupled-spin metabolites vary with changing TE due to the effects of J evolution as well as the transverse relaxation. Therefore, when basis spectra that include the J evolution effects are used for spectral fitting on multi-TE data, the relaxation time constant can be obtained directly from the TE dependence of the spectral fitting estimates. Moreover, for spectra obtained with PRESS volume localization, the signals of coupled resonances are largely affected by the 180° pulses. The effects of the finite bandwidth and imperfect refocusing profile have to be taken into account to evaluate the scalar coupling effects on the signals. This was accomplished incorporating the actual RF pulse waveforms in calculating the basis spectra in the present study.

The four TEs used in this study appear to be reasonably optimal for $T_2^\dagger$ estimation of Glu and mIns in the human brain. Although the shortest TE (54 ms) may not be sufficiently long for complete suppression of macromolecule signals, spectral fitting using precisely-calculated basis spectra differentiated effectively the metabolite signals from the residual macromolecule signals, leading to Glu and mIns CRLBs smaller than those at short TEs in prior studies at the same field strength (23,24). At long TEs, the metabolite signals were attenuated substantively, but using the proper basis spectra the CRLBs of Glu and mIns of the present study were comparable to those of the prior short-TE studies (≤ 10%). The resonances of Gln are proximate to the Glu resonances, but the Gln signals were resolvable with CRLB < 20% at TEs 54, 112, and 264 ms (mean CRLB = 12±4%, 11±4%, and 8±3% (n = 10), respectively). The Gln signal at TE = 374 was not properly measurable (CRLB > 100%) likely due to the insufficient SNR. Given that the precision of signal estimates is governed by SNR and critical for relaxation time estimation, measurements at the four TEs with various number of averages allowed us to achieve acceptable precision of LCModel estimates and $T_2^\dagger$ values for several J-coupled metabolites, as indicated by the R^2 values comparable to those in recent T_2 studies with greater number of TEs (12,14,17). Despite the increased number of signal averaging at the long TE (128 averages), the CRLBs of mIns at TE = 374 ms were relatively large (9.1±2.0%, N=10) due to the extensive signal degradation arising from the J coupling effects (Fig. 4).

The estimated $T_2^\dagger$ values of the present study may well be apparent relaxation time constants, presumably specific to the PRESS sequence used. With the changing inter-RF pulse delays for multi-TE measurements, the relaxation estimates may include the effects of spin-spin relaxation (T_2) and molecular diffusion under the field gradients created by magnetic susceptibility distribution, thereby resulting in $T_2^\dagger < T_2$. The T_2 of brain metabolites may be measured employing constant, short inter-RF pulse delays in multi-TE scans *in vivo* (11). In the present study, signal reduction due to diffusion under spoiling gradient pulses may be minimal and equal at all TEs since the diffusivity of metabolites in the human brain is low ($< 0.3\times10^{-7}$ m^2/s) (25) and the inter-gradient pulse intervals were relatively short (~17 ms) and kept constant in the multi-TE scans. The molecular diffusion effects associated with the pulsed field gradient pulses may therefore be negligible in our

relaxation estimates. In addition, the use of constant TR of 3 s for the multi-TE scans may lead to relaxation estimates shorter than the T_2. However, this effect does not seem substantial. The trajectory of the longitudinal magnetization in the steady-state condition ($TR < 5\times T_1$) is varied with changing TE, resulting in unequal initial longitudinal magnetization prior to the 90° excitation in multi-TE scans (26). Assuming that for a PRESS sequence the ratio of the steady-state initial longitudinal magnetization to the thermal equilibrium magnetization is given by $1 - E_{TR} + 2E_{TR}E_1 - 2E_{TR}E_2$, where $E_{TR} = exp(-TR/T_1)$, $E_1 = exp((TE_1/2)/T_1)$, and $E_2 = exp((TE_1 + TE_2/2)/T_1)$, the $T_2^{\dagger}$ estimates can be corrected for constant-TR effects using known T_1 values. For published T_1 of ~1.2 s for Glu and mIns at 3T (9,12), the steady-state constant-TR effect on the $T_2^{\dagger}$ estimates of the present study is predicted to be only 1.5% compared to $T_2^{\dagger}$ estimates from $TR \gg T_1$. For tCr and NAA with T_1 of ~1.4 s, the discrepancy may be 1.6%.

Prior studies of relaxation time measurements for brain metabolites indicated consistently that $T_2^{\dagger}$ of the NAA singlet differs between gray and white matter (9,12,14,15). The $T_2^{\dagger}$s of the NAA singlet from the medial occipital and left occipital regions in the present study were similar to those of the prior studies for occipital GM and WM (9,12), indicating that GM and WM were dominant in the voxels positioned in the medial occipital and left occipital cortices in the present study, respectively, in agreement with the GM, WM and CSF estimates shown earlier. The NAA-Asp CH_2 multiplet also showed $T_2^{\dagger}$ longer in left occipital than in medial occipital, most likely due to the different fractions of GM and WM within the voxels. The NAA-Asp $T_2^{\dagger}$ was measured separately from the NAA singlet. While it is necessary to individually fit the subgroups of metabolites to take into account possible differences in relaxation times between resonances within a metabolite, this approach may decrease the precision of spectral fitting. The NAAG signals from the left occipital region were measurable with CRLB < 20% at the four TEs, most likely because of its relatively high concentration in WM compared to that in GM, as indicated by prior studies (27,28). For the medial occipital cortex, CRLB of NAAG was less than 20% at TEs other than the longest TE in 4 subjects. Monoexponential fitting of the data at the three TEs gave an NAAG $T_2^{\dagger}$ of 252±49 ms, implying that the NAAG relaxation time may differ between GM and WM, similarly to NAA.

The $T_2^{\dagger}$ of Glu in the GM and WM dominant regions in the human brain was estimated to be about the same in the present study (180 ms), similarly to a prior study (16), but somewhat shorter than the previously reported value (200 ms). Although the investigated brain regions differ (occipital *vs*. frontal), given that the metabolite $T_2^{\dagger}$ estimation depends on the number of refocusing RF pulses (11), the difference in Glu $T_2^{\dagger}$s from the two studies may be in part due to the difference in the effects of inter-RF pulse molecular diffusion during the sequences (dual refocusing *vs*. triple refocusing). Presumably for a similar reason, the tCr-CH_3 $T_2^{\dagger}$ was shorter in the present study (~150 ms) than in the prior triple-refocusing study (~165 ms). In the present study, Glu $T_2^{\dagger}$ was measured to be much shorter than NAA-CH_3 $T_2^{\dagger}$ (~290 ms). The large $T_2^{\dagger}$ difference between Glu and NAA was also the case in phantom solutions (~700 *vs*. 1200 ms). These *in vivo* and phantom results may be as expected given that the CH_2 protons (Glu) are most likely less mobile than the CH_3 protons (NAA) and consequently the motional averaging of the dipole-dipole interaction occurs less in Glu than in NAA. In the brain, Glu and NAA are largely present within neuronal cells and the intra-molecular dipolar interaction may be a dominant mechanism for T_2 relaxation in both Glu and NAA. However, for tCr, the $T_2^{\dagger}$ (3.02 ppm) was shorter than the NAA-CH_3 $T_2^{\dagger}$ in many prior studies (7–15) and in the present study. This may not be due to the difference in the diffusion-induced dynamic dephasing since the diffusion constants of tCr and NAA are similar (29–31). The relatively short $T_2^{\dagger}$ of tCr may be a result of tCr-to-water magnetization transfer occurring *via* immobile proton pools (32,33). Since in all prior and present T_2 studies the data were acquired following water suppression (*i.e.*, creation of large

magnetization difference between the tCr and water proton pools with respect to their thermal equilibrium values), the tCr signals may undergo further relaxation with increasing TE in addition to the relaxation caused by the intra-molecular dipolar interaction, thereby leading to reduced $T_2^{\dagger}$, shorter than that of Glu $T_2^{\dagger}$, as in the present and prior Glu T_2 studies. The tCr $T_2^{\dagger}$ may become longer when measured without water suppression. In phantom solutions, in which the magnetization transfer is not present, the Cr-CH_3 and NAA-CH_3 $T_2^{\dagger}$s are similar due to the similarity in their dipolar interaction strength. For the brain water (excluding CSF), the $T_2^{\dagger}$ was measured to be short (~80 ms) compared to metabolite $T_2^{\dagger}$ because of the strong intra-molecular interactions and the high diffusivity in water (29–31).

In conclusion, we have demonstrated measurement of apparent proton T_2 of coupled-spin metabolites in the human brain using a PRESS sequence at 3T *in vivo*. The signals of brain metabolites, including Glu, mIns and NAAG, were resolved, for the GM-dominant medial occipital and WM-dominant left occipital regions, at four selected echo times using spectral fitting with numerically calculated basis spectra. Further studies will be required to determine variations in relaxation times across brain regions and in disease conditions.

Acknowledgments

Grants: Cancer Prevention Research Institute of Texas (CPRIT) (RP101243-P04)

National Institute of Health (RC1NS0760675)

National Center for Research Resources (P41 RR002584)

Abbreviations

PRESS	point-resolved spectroscopy
STEAM	stimulated-echo acquisition mode
CRLB	Cramér Rao lower bound
SD	standard deviation
SNR	signal-to-noise ratio
RF	radio-frequency
FASTMAP	fast automatic shimming technique by mapping along projections
Cr	creatine
Glu	glutamate
Gln	glutamine
GSH	glutathione
GABA	γ-aminobutyric acid
GPC	glycerophosphocholine
PC	phosphocholine
mIns	myo-inositol
NAA	N-acetylasparate
NAAG	N-acetlyaspartylglutamate
Asp	aspartate

References

1. Schubert F, Gallinat J, Seifert F, Rinneberg H. Glutamate concentrations in human brain using single voxel proton magnetic resonance spectroscopy at 3 Tesla. Neuroimage. 2004; 21:1762–1771. [PubMed: 15050596]
2. Coupland NJ, Ogilvie CJ, Hegadoren KM, Seres P, Hanstock CC, Allen PS. Decreased prefrontal Myo-inositol in major depressive disorder. Biol Psychiatry. 2005; 57:1526–1534. [PubMed: 15953489]
3. Purdon SE, Valiakalayil A, Hanstock CC, Seres P, Tibbo P. Elevated 3T proton MRS glutamate levels associated with poor Continuous Performance Test (CPT-0X) scores and genetic risk for schizophrenia. Schizophr Res. 2008; 99:218–224. [PubMed: 18248960]
4. Frahm J, Bruhn H, Gyngell ML, Merboldt KD, Hanicke W, Sauter R. Localized proton NMR spectroscopy in different regions of the human brain in vivo. Relaxation times and concentrations of cerebral metabolites. Magn Reson Med. 1989; 11:47–63. [PubMed: 2747516]
5. Kreis R, Ernst T, Ross BD. Development of the human brain: in vivo quantification of metabolite and water content with proton magnetic resonance spectroscopy. Magn Reson Med. 1993; 30(4): 424–437. [PubMed: 8255190]
6. Ongur D, Prescot AP, Jensen JE, Rouse ED, Cohen BM, Renshaw PF, Olson DP. T_2 relaxation time abnormalities in bipolar disorder and schizophrenia. Magn Reson Med. 2010; 63:1–8. [PubMed: 19918902]
7. Hetherington HP, Mason GF, Pan JW, Ponder SL, Vaughan JT, Twieg DB, Pohost GM. Evaluation of cerebral gray and white matter metabolite differences by spectroscopic imaging at 4.1T. Magn Reson Med. 1994; 32:565–571. [PubMed: 7808257]
8. Posse S, Cuenod CA, Risinger R, Le Bihan D, Balaban RS. Anomalous transverse relaxation in 1H spectroscopy in human brain at 4 Tesla. Magn Reson Med. 1995; 33:246–252. [PubMed: 7707916]
9. Mlynarik V, Gruber S, Moser E. Proton T_1 and T_2 relaxation times of human brain metabolites at 3 Tesla. NMR Biomed. 2001; 14:325–331. [PubMed: 11477653]
10. Barker PB, Hearshen DO, Boska MD. Single-voxel proton MRS of the human brain at 1.5T and 3.0T. Magn Reson Med. 2001; 45:765–769. [PubMed: 11323802]
11. Michaeli S, Garwood M, Zhu XH, DelaBarre L, Andersen P, Adriany G, Merkle H, Ugurbil K, Chen W. Proton T_2 relaxation study of water, N-acetylaspartate, and creatine in human brain using Hahn and Carr-Purcell spin echoes at 4T and 7T. Magn Reson Med. 2002; 47:629–633. [PubMed: 11948722]
12. Traber F, Block W, Lamerichs R, Gieseke J, Schild HH. 1H metabolite relaxation times at 3.0 tesla: Measurements of T_1 and T_2 values in normal brain and determination of regional differences in transverse relaxation. J Magn Reson Imaging. 2004; 19:537–545. [PubMed: 15112302]
13. Brief EE, Whittall KP, Li DK, MacKay AL. Proton T_2 relaxation of cerebral metabolites of normal human brain over large TE range. NMR Biomed. 2005; 18:14–18. [PubMed: 15455460]
14. Tsai SY, Posse S, Lin YR, Ko CW, Otazo R, Chung HW, Lin FH. Fast mapping of the T_2 relaxation time of cerebral metabolites using proton echo-planar spectroscopic imaging (PEPSI). Magn Reson Med. 2007; 57:859–865. [PubMed: 17457864]
15. Zaaraoui W, Fleysher L, Fleysher R, Liu S, Soher BJ, Gonen O. Human brain-structure resolved T_2 relaxation times of proton metabolites at 3 Tesla. Magn Reson Med. 2007; 57:983–989. [PubMed: 17534907]
16. Choi C, Coupland NJ, Bhardwaj PP, Kalra S, Casault CA, Reid K, Allen PS. T_2 measurement and quantification of glutamate in human brain in vivo. Magn Reson Med. 2006; 56:971–977. [PubMed: 17029225]
17. Xin L, Gambarota G, Mlynarik V, Gruetter R. Proton T_2 relaxation time of J-coupled cerebral metabolites in rat brain at 9.4 T. NMR Biomed. 2008; 21:396–401. [PubMed: 17907262]
18. Govindaraju V, Young K, Maudsley AA. Proton NMR chemical shifts and coupling constants for brain metabolites. NMR Biomed. 2000; 13:129–153. [PubMed: 10861994]
19. Slotboom J, Mehlkope AF, Bovee WMMJ. The effects of frequency-selective RF pulses on J-coupled spin-1/2 systems. J Magn Reson A. 1994; 108:38–50.

20. Choi C, Dimitrov I, Douglas D, Zhao C, Hawesa H, Ghose S, Tamminga CA. In vivo detection of serine in the human brain by proton magnetic resonance spectroscopy (1H-MRS) at 7 Tesla. Magn Reson Med. 2009; 62:1042–1046. [PubMed: 19526507]
21. Gruetter R. Automatic, localized in vivo adjustment of all first- and second-order shim coils. Magn Reson Med. 1993; 29:804–811. [PubMed: 8350724]
22. Provencher SW. Estimation of metabolite concentrations from localized in vivo proton NMR spectra. Magn Reson Med. 1993; 30:672–679. [PubMed: 8139448]
23. Gottschalk M, Lamalle L, Segebarth C. Short-TE localised ^{1}H MRS of the human brain at 3 T: quantification of the metabolite signals using two approaches to account for macromolecular signal contributions. NMR Biomed. 2008; 21:507–517. [PubMed: 17955570]
24. Mullins PG, Chen H, Xu J, Caprihan A, Gasparovic C. Comparative reliability of proton spectroscopy techniques designed to improve detection of J-coupled metabolites. Magn Reson Med. 2008; 60:964–969. [PubMed: 18816817]
25. Posse S, Cuenod CA, Le Bihan D. Human brain: proton diffusion MR spectroscopy. Radiology. 1993; 188:719–725. [PubMed: 8351339]
26. Redpath TW, Smith FW. Technical note: use of a double inversion recovery pulse sequence to image selectively grey or white brain matter. Br J Radiol. 1994; 67:1258–1263. [PubMed: 7874427]
27. Pouwels PJ, Frahm J. Differential distribution of NAA and NAAG in human brain as determined by quantitative localized proton MRS. NMR Biomed. 1997; 10:73–78. [PubMed: 9267864]
28. Choi C, Ghose S, Uh J, Patel A, Dimitrov IE, Lu H, Douglas D, Ganji S. Measurement of N-acetylaspartylglutamate in the human frontal brain by ^{1}H-MRS at 7T. Magn Reson Med. 2010; 64:1247–1251. [PubMed: 20597122]
29. de Graaf RA, Braun KP, Nicolay K. Single-shot diffusion trace ^{1}H NMR spectroscopy. Magn Reson Med. 2001; 45:741–748. [PubMed: 11323799]
30. Ellegood J, Hanstock CC, Beaulieu C. Trace apparent diffusion coefficients of metabolites in human brain using diffusion weighted magnetic resonance spectroscopy. Magn Reson Med. 2005; 53:1025–1032. [PubMed: 15844150]
31. Nicolay K, Braun KP, Graaf RA, Dijkhuizen RM, Kruiskamp MJ. Diffusion NMR spectroscopy. NMR Biomed. 2001; 14:94–111. [PubMed: 11320536]
32. Dreher W, Norris DG, Leibfritz D. Magnetization transfer affects the proton creatine/phosphocreatine signal intensity: in vivo demonstration in the rat brain. Magn Reson Med. 1994; 31:81–84. [PubMed: 8121275]
33. Meyerhoff DJ. Proton magnetization transfer of metabolites in human brain. Magn Reson Med. 1999; 42:417–420. [PubMed: 10467283]

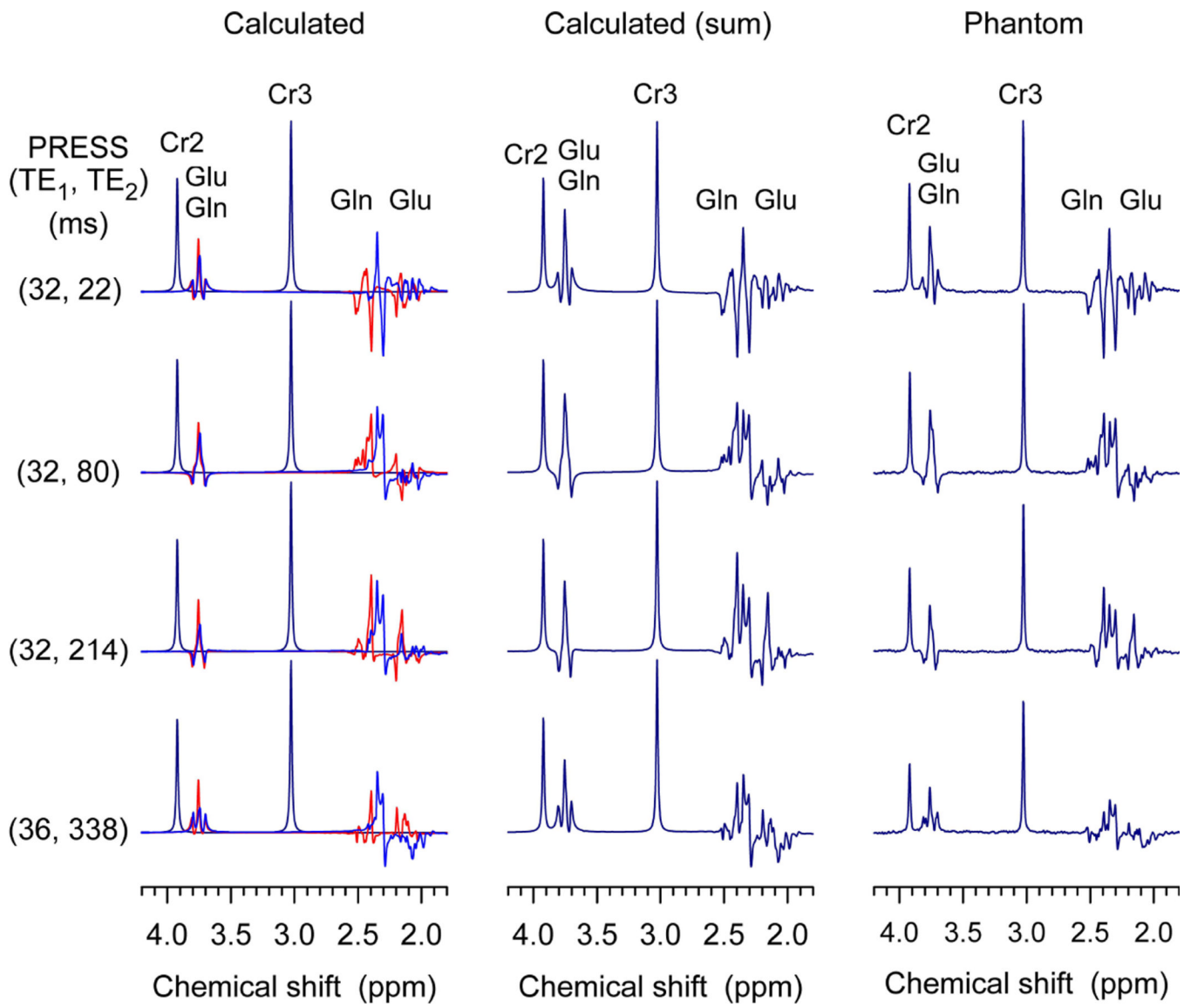

Figure 1.

Comparison between numerically calculated and phantom spectra of Glu (20 mM), Gln (20 mM), and Cr (8 mM) for the four pairs of PRESS subecho times (TE_1, TE_2) used for *in vivo* T_2 measurements. Spectra were broadened to 2.5 Hz. Spectra were calculated ignoring the signal reduction due to T_2 effects.

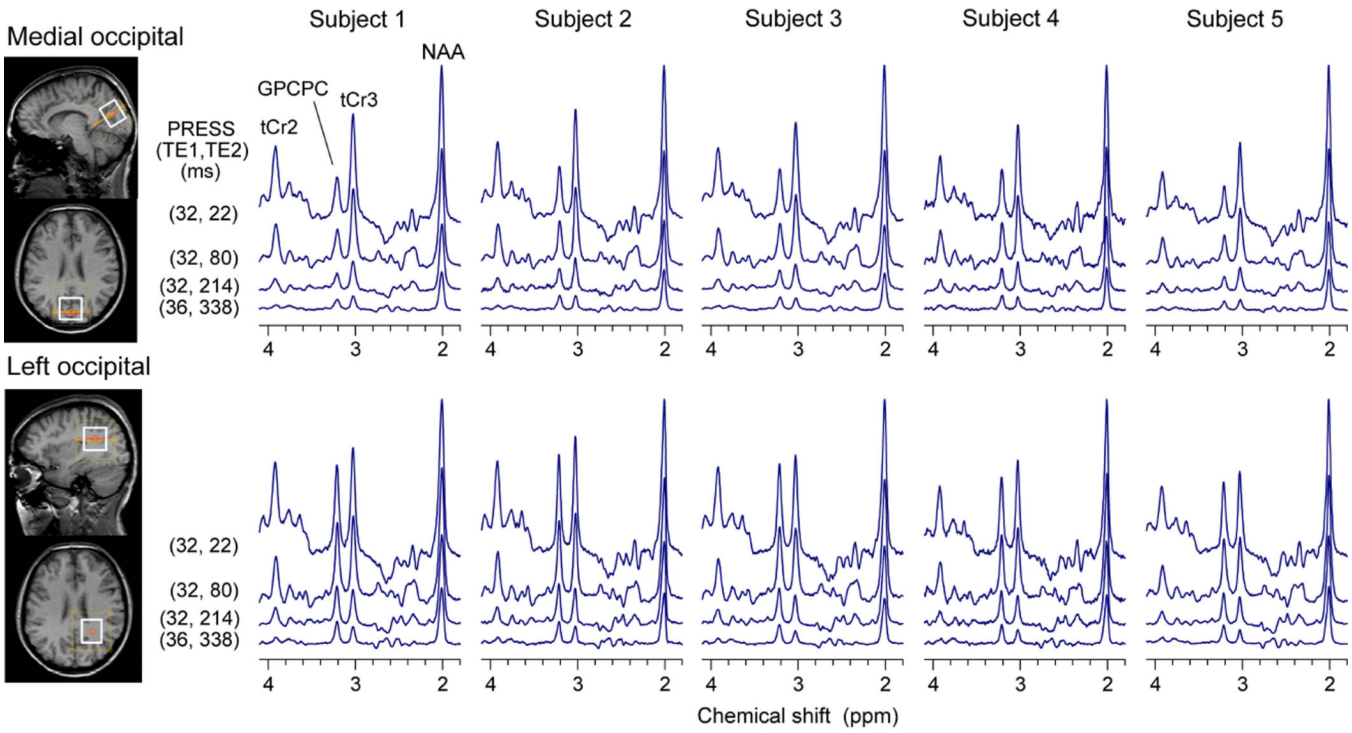

Figure 2.

In vivo spectra, at the four (TE_1, TE_2) pairs of PRESS, from medial occipital and left occipital cortices of five healthy volunteers are presented together with voxel positioning (size 25×30×30 mm^3). Spectra are normalized with respect to the NAA singlet at TE = 54 ms for each brain region. FIDs were filtered with a 1-Hz exponential function prior to the Fourier transformation. The number of signal averages was 16, 32, 64, and 128 for TE = 54, 112, 246, and 374 ms, respectively (TR = 3 s).

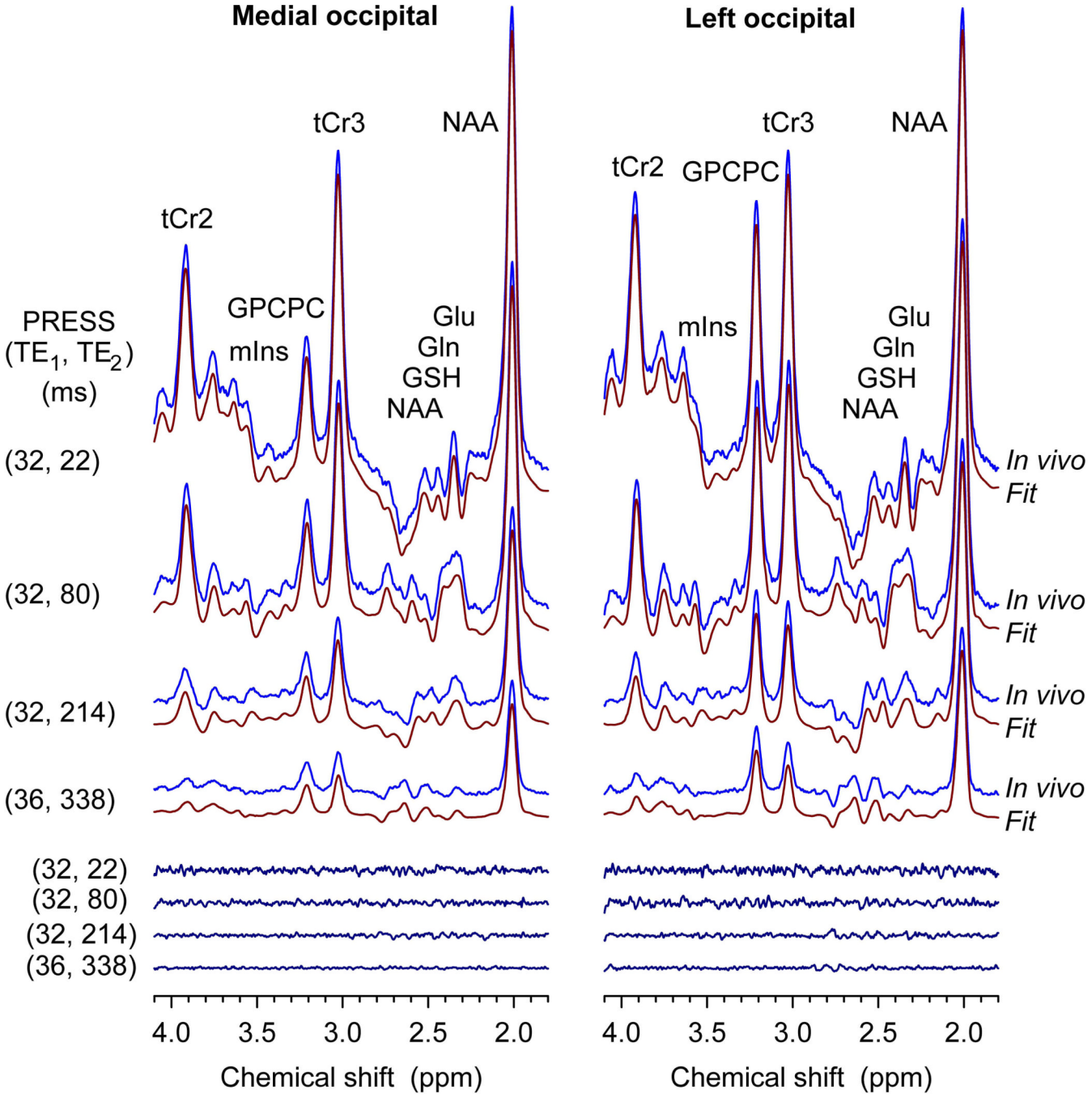

Figure 3.

In vivo spectra at the four (TE_1, TE_2) pairs of PRESS from medial occipital and left occipital cortices of a healthy volunteer (subject 1 in Fig. 2) are shown together with LCModel fits and residuals. The decreasing residual levels with increasing TE are due to the different number of signal averages (16, 32, 64, and 128, top to bottom). Spectra are normalized with respect to the NAA singlet at TE = 54 ms for each voxel.

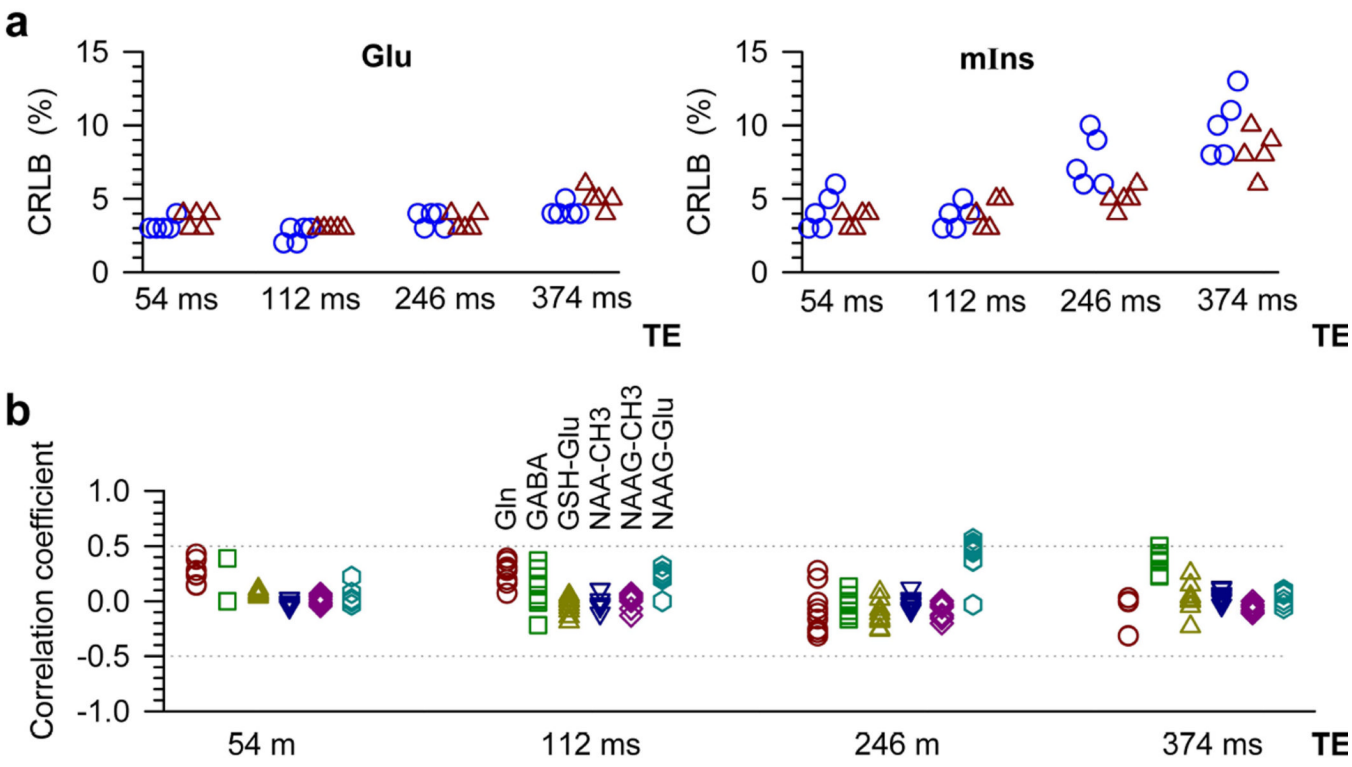

Figure 4.

(a) The CRLBs of Glu and mIns are shown for the four TEs used for T_2† **measurement. For each TE**, five data points on left (circle) represent CRLBs in spectra from medial occipital, and five data points on right (triangle) from left occipital. (**b**) The correlation coefficients, returned by LCModel, between Glu and metabolites having resonances in the proximity of the Glu signals. The metabolites include Gln (circle), GABA (square), GSH Glu moiety (triangle up), NAA-CH_3 (triangle down), NAAG-CH_3 (diamond), and NAAG Glu moiety (hexagon).

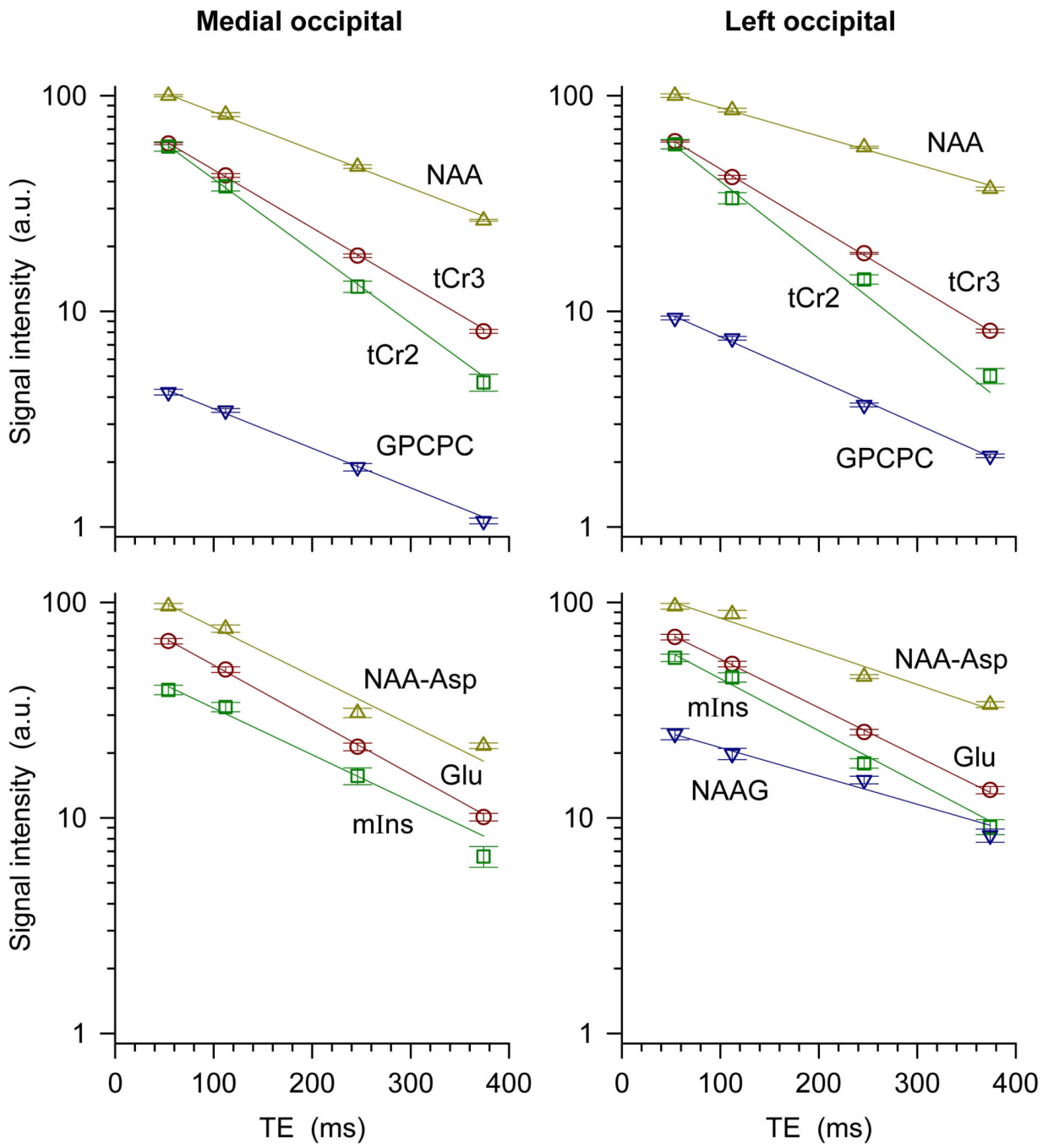

Figure 5.
Monoexponential fitting of LCModel estimates *vs*. TE (= TE_1 + TE_2) for the medial occipital and left occipital lobes. The upper panel shows fits of major singlet signals (tCr-CH_3, tCr-CH_2, NAA and GPCPC) and the lower panel shows fits of major multiplets (Glu, mIns and the NAA aspartate moiety) and the NAAG singlet (left occipital only). Error bars indicate the standard deviation of the LCModel estimates.

Table 1

Apparent T_2 ($T_2^\dagger$) values and the coefficients of determination (R^2) of monoexponential fitting of metabolites and water data from the medial occipital and left occipital cortices are shown together with *p*-values for $T_2^\dagger$ differences between the two brain regions. The Bonferroni-corrected *p*-values were obtained by multiplying the uncorrected *p*-values by the number of metabolites (*i.e.*, 7, excluding NAAG). When the Bonferroni-corrected *p*-value was greater than one, the *p* value was set to 1. The water $T_2^\dagger$ was estimated from the signals at TE = 54, 112, and 246 ms. $T_2^\dagger$ and R^2 are mean±SD (N=5).

	Medial occipital		**Left occipital**		**Paired t-test**	**Bonferroni corrected**
	$T_2^\dagger$ (ms)	**R^2**	**$T_2^\dagger$ (ms)**	**R^2**	***p***	***p***
tCr-CH_3	147±10	0.998	156±7	0.998	0.0839	0.5873
tCr-CH_2	124±6	0.998	123±11	0.998	0.8730	1
NAA	258±11	0.995	309±16	0.989	0.0078	0.0545
GPCPC	241±13	0.981	224±15	0.993	0.2169	1
Glu	181±16	0.996	180±12	0.994	0.8809	1
mIns	197±14	0.977	196±17	0.983	0.9342	1
NAA-Asp	222±33	0.986	284±23	0.963	0.0094	0.0657
NAAG	-	-	292±35	0.934	-	-
Water	83±7	0.998	83±5	0.999	0.9884	-

NMR Biomed. Author manuscript; available in PMC 2013 December 05.